

## Band-stop optical nanofilters with split-ring resonators based on metal-insulator-metal structure

This content has been downloaded from IOPscience. Please scroll down to see the full text.

2014 Chinese Phys. B 23 097301

(<http://iopscience.iop.org/1674-1056/23/9/097301>)

View [the table of contents for this issue](#), or go to the [journal homepage](#) for more

Download details:

IP Address: 115.156.166.253

This content was downloaded on 12/12/2014 at 14:06

Please note that [terms and conditions apply](#).

# Band-stop optical nanofilters with split-ring resonators based on metal–insulator–metal structure\*

Zhang Hui-Yun(张会云)<sup>a)</sup>, Shen Duan-Long(申端龙)<sup>a)</sup>, Zhang Yu-Ping(张玉萍)<sup>a)†</sup>, Yang Wei-Jie(杨伟杰)<sup>b)</sup>, Yuan Cai(袁 恺)<sup>c)</sup>, Liu Meng(刘 蒙)<sup>a)</sup>, Yin Yi-Heng(尹贻恒)<sup>a)</sup>, and Wu Zhi-Xin(吴志心)<sup>a)</sup>

<sup>a)</sup>Qingdao Key Laboratory of Terahertz Technology, College of Electronics, Communication, and Physics, Shandong University of Science and Technology, Qingdao 266590, China

<sup>b)</sup>Dongjun Information Technology Co., Ltd., Shanghai 200050, China

<sup>c)</sup>College of Precision Instrument and Opto-electronics Engineering, Institute of Laser and Opto-electronics, Tianjin University, Tianjin 300072, China

(Received 17 December 2013; revised manuscript received 30 March 2014; published online 16 July 2014)

Novel band-stop filters with circular split-ring resonators based on the metal–insulator–metal (MIM) structure are presented, with their transmission properties of SPPs propagating through the filter simulated by the finite-difference time-domain (FDTD) method. The variation of the gap of the split ring can affect the transmission characteristics, i.e., the transmission spectrum of SPPs exhibiting a shift, which is useful for modulating the filter. Linear and nonlinear media are used in the resonator respectively. By varying the refractive index of the linear medium, the transmission properties can be changed obviously, and the effect caused by changing the incident intensity with a nonlinear medium is similar. Several resonant modes that are applicable can be enhanced by changing the position of the gap of the split ring. Thus, the transmission properties can be modulated by adjusting the size of the gap, varying the refractive index, and changing the incident intensity of the input light. These methods may play significant roles in applications of optical integrated circuits and nanostructural devices.

**Keywords:** surface plasmons, nano filter, split-ring resonator, transmission property

**PACS:** 73.20.Mf, 78.20.Bh, 43.58.Kr

**DOI:** 10.1088/1674-1056/23/9/097301

## 1. Introduction

Surface plasmon polaritons (SPPs) have been widely studied because of their special properties and potential applications in the field of nano science and sub-wavelength photonic devices. SPPs can be excited by coupling light waves with a special metal nanostructure,<sup>[1]</sup> then they will be confined to the sub-wavelength scale in the metal nanostructure and controlled by the surface characteristics, finally, they will be converted into optical waves as an output from the nanostructure. The nano-scale structure can be used to overcome the limitations of the traditional optical devices, for example, the diffraction limit of the electromagnetic wave in the small scale. Devices based on SPPs have been studied and applied extensively in recent years, such as the Bragg reflector,<sup>[2]</sup> the sub-wavelength beam manipulation,<sup>[3]</sup> the plasmon optical switch,<sup>[4]</sup> the Mach–Zehnder interferometer,<sup>[5]</sup> the single metal wire,<sup>[6]</sup> and the SPP waveguides.<sup>[7]</sup> The SPP waveguides based on metal–insulator–metal (MIM) structures have been discussed, in which the resonator is designed with different geometry structures, such as circular ring,<sup>[8–11]</sup> rectangular ring,<sup>[12–14]</sup> and tooth-shaped plasmonic waveguide.<sup>[15]</sup> Those waveguides can be used as filters in the nanometer scale with different filtering characteristics depending on the rela-

tive positions between the waveguides and the resonators. It is used as a band-pass filter when putting the resonator between the input and the output waveguides.<sup>[9,11–13,16–19]</sup> Wang *et al.* have investigated a two-dimensional (2D) plasmonic structure composed of two straight MIM waveguides and one circular ring resonator between them,<sup>[9]</sup> and showed that the wavelengths for the maximum transmittance can be shifted by varying the radius of the ring. In another band-pass filter with a hollow-core rectangular ring resonator between the two waveguides,<sup>[13]</sup> the resonant wavelengths shift towards the long wavelength by increasing the dimension of the hollow core. By placing the resonator beside the bus waveguide, the device can be used as a band-stop filter.<sup>[8,10,14,18,19]</sup> Channel drop filters with disk/ring resonators have also been investigated,<sup>[8]</sup> in which the light can be dropped efficiently. Hosseini *et al.* designed a resonator using a rectangular geometry.<sup>[20]</sup> In the optical filter with rectangular split-ring resonators proposed in the literature,<sup>[21,22]</sup> the resonant wavelengths vary depending on the position and the size of the gap.

In this paper, a novel MIM structure of a band-stop plasmonic filter with a circular split-ring resonator is proposed, with dielectric filling in the air groove. The transmission characteristics are studied in several different cases with split gaps

\*Project supported by the National Natural Science Foundation of China (Grant No. 61001018), the Natural Science Foundation of Shandong Province, China (Grant Nos. ZR2011FM009 and ZR2012FM011), the Research Fund of Shandong University of Science and Technology (SDUST), China (Grant No. 2010KYJQ103), the SDUST Research Fund, China (Grant No. 2012KYTD103), the Shandong Province Higher Educational Science and Technology Program, China (Grant No. J11LG20), and the Qingdao Economic & Technical Development Zone Science & Technology Project, China (Grant No. 2013-1-64).

†Corresponding author. E-mail: [sdust\\_thz@163.com](mailto:sdust_thz@163.com)

at different positions and dielectrics of different permittivities using the finite-difference time-domain (FDTD) method. Based on the result, a novel method is proposed to modulate the resonant wavelengths effectively in the nano scale. Band-stop filters with closed circular<sup>[8,23]</sup> or rectangular<sup>[14,20]</sup> ring resonators are studied; different filter characteristics can be obtained by varying the refractive index of the medium, the size of the resonators, the distance between the bus waveguide and the resonator, and so on. With the split rings proposed in this paper, the filters can be tuned by using more active methods due to the existence of the gap. By varying the positions of the gap, the resonant strength of the absorption peak can be stronger. The tuning range can be wider by adjusting the width of the gap, the refractive index of the medium, or the strength of the incident light.

## 2. Model and theory

An MIM nanostructure with a split-ring resonator is shown in Fig. 1. The gray part shows the metallic silver, while the waveguide and the ring are insulators and are set to be air or dielectric. A metal wall (gap of the ring) is positioned as shown in the figure with width  $w$ . The waveguide and the circular passage have equal width, which is much smaller than the wavelengths and set to be 50 nm in our case. The outer radius of the ring is  $r_o = 150$  nm, and the inner radius is  $r_i = 100$  nm. The distance between the resonator and the bus waveguide,  $s$ , is set to be 10 nm. Two power monitors are placed at points  $P$  and  $Q$  to detect the incident power  $P_{in}$  and the transmitted power  $P_{out}$ , and the transmittance is defined as  $T = P_{out}/P_{in}$ .

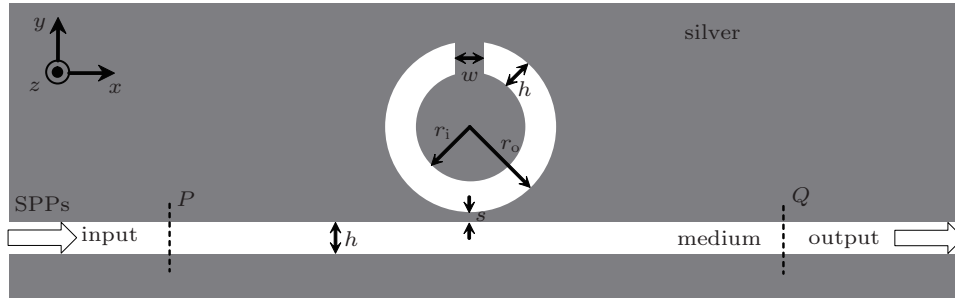


Fig. 1. Schematic diagram of the plasmonic band-stop filter with an MIM structure.

The dispersion relation of SPPs can be expressed as<sup>[9]</sup>

$$\tanh\left(\frac{h}{2}k_0\sqrt{n_{\text{eff}}^2 - \epsilon_0}\right) = -\frac{\epsilon_0\sqrt{n_{\text{eff}}^2 - \epsilon_m}}{\epsilon_m\sqrt{n_{\text{eff}}^2 - \epsilon_0}}, \quad (1)$$

where  $n_{\text{eff}} = \beta/k_0$  is the effective refraction index of the SPPs,  $\beta$  and  $k_0$  are the propagation constants of the SPPs and the free space, respectively,  $\epsilon_0$  is the permittivity of air, and  $\epsilon_m$  is the permittivity of the metal. The Lorentz model is often used to characterize the frequency-dependent complex permittivity of the silver<sup>[24]</sup>

$$\epsilon_m(\omega) = \epsilon_\infty + \sum_m \frac{\omega_{p,m}^2}{\omega_{a,m}^2 - \omega^2 - i\omega\omega_{c,m}}, \quad (2)$$

where  $\epsilon_\infty$  is the relative permittivity at infinite frequency, it approximately equals to 1 when the frequency is low enough;  $\omega_a$  is the resonant frequency;  $\omega_p$  is the plasmon frequency of the metal; and  $\omega_c$  is the collision frequency of the electrons in the metal, which is also called the damping constant. The permittivity spectrum is plotted in Fig. 2(a), with all the parameters consistent with those in Ref. [24]. In this case, by considering the first term of the summation and neglecting the other terms,  $\omega_a$  equals to 0. The model is simplified to the Drude model for

the frequency-dependent complex permittivity of the silver. It can be expressed by the following formula:

$$\epsilon_m(\omega) = \epsilon_\infty - \frac{\omega_p^2}{\omega^2 + i\omega\omega_c}. \quad (3a)$$

Separating the real and the imaginary parts yields

$$\epsilon_m(\omega) = \epsilon_\infty - \frac{\omega_p^2}{\omega^2 + \omega_c^2} + i\frac{\omega_p^2\omega_c}{\omega^3 + \omega_c^2\omega}, \quad (3b)$$

where  $\epsilon_\infty = 1$ ,  $\omega_c = 27.3$  THz, and  $\omega_p = 2196.3$  THz. The permittivity spectrum of the Drude model is plotted in Fig. 2(b). The Drude model, which is adopted in this research, can be regarded as a special form of the Lorentz model and is suitable for describing the actual metal.

The FDTD method is adopted to investigate the transmission characteristics of the structure. In the simulations, the grid sizes along the  $x$  and  $y$  directions are set to be  $\Delta x = \Delta y = 5$  nm, and the time step is set to be  $\Delta t = \Delta x/2c$ , where  $c$  is the velocity of light in a vacuum. The computational space is surrounded by open boundary conditions of impedance matching absorption in the  $x$  direction and periodic boundary conditions in the  $y$  and  $z$  directions.

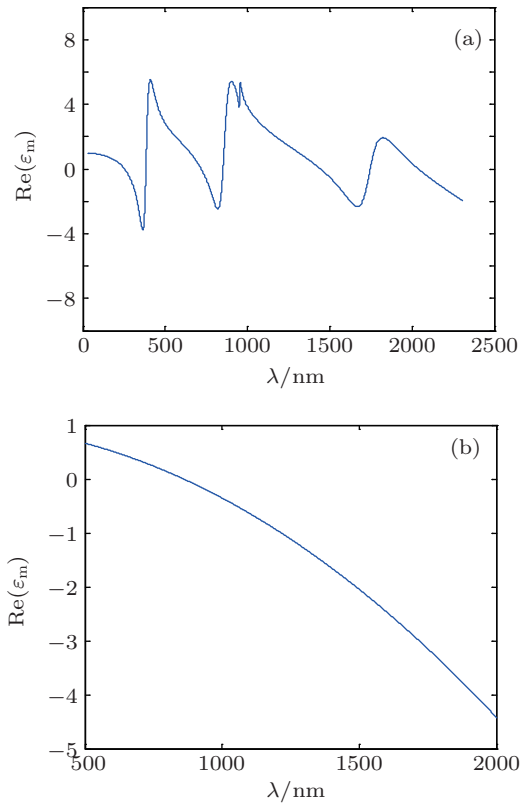


**Fig. 2.** (color online) Dependence of  $\text{Re}(\epsilon_m)$  of silver on the wavelength of the incident light in (a) the Lorentz model, and (b) the Drude model.

### 3. Simulation and results

#### 3.1. MIM band-stop filters with different metal wall widths

An MIM band-stop filter with a circular split-ring resonator full of air is shown in Fig. 3, with SPPs propagating in the bus waveguide. A resonance effect occurs when the SPPs propagate through the bus waveguide, hence the transmittances at several special wavelengths will drop obviously due to the resonance. The resonant wavelength is determined by the resonance condition

$$L_{\text{eff}} n_{\text{eff}} = N\lambda, \quad N = 1, 2, 3, \dots, \quad (4)$$

where  $L_{\text{eff}}$  is the effective length of the split ring and  $n_{\text{eff}}$  is the effective refractive index of the SPPs. For simplicity, the effective refractive index is assumed to be related to the width of the MIM waveguide and the permittivities of the air and the metal, as shown in formula (1).

The transmittance of the SPPs propagating through the filter with different gap widths is shown in Fig. 4. It can be found that the resonant wavelengths of the filter move in the short-wavelength direction when  $w$  is increased from 20 nm to 100 nm, which is called the blue shift. For a given cavity size (certain effective length of the split ring), resonant waves with corresponding wavelengths can be generated, which resonate with the waves at the same wavelengths in the bus waveguide. These waves at the resonant modes in the bus waveguide cannot propagate through the waveguide, so several absorption

peaks appear on the spectrum. The effective length  $L_{\text{eff}}$  decreases with the increase of the width of the wall, thus, for the same resonance mode ( $N$  remains unchanged), the resonance wavelength becomes shorter accordingly, and the blue shift appears. The transmission spectrum can be tuned continuously by varying the width of the wall, as shown in Fig. 4(a). Figure 4(b) shows that the wavelength at the different transmission valley depends on the width of the wall. In this device, the major part of the input spectrum will pass through the filter, with only a few resonant wavelengths held back, so it is called a band-stop filter. The chosen metal is silver in this case, the medium is air, and the width of the metal wall is set to be 20 nm, 40 nm, 60 nm, 80 nm, or 100 nm.

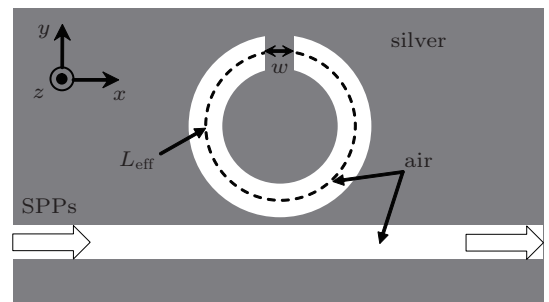


**Fig. 3.** Structure of the filter with a split-ring resonator filled with air coupled with a bus waveguide.

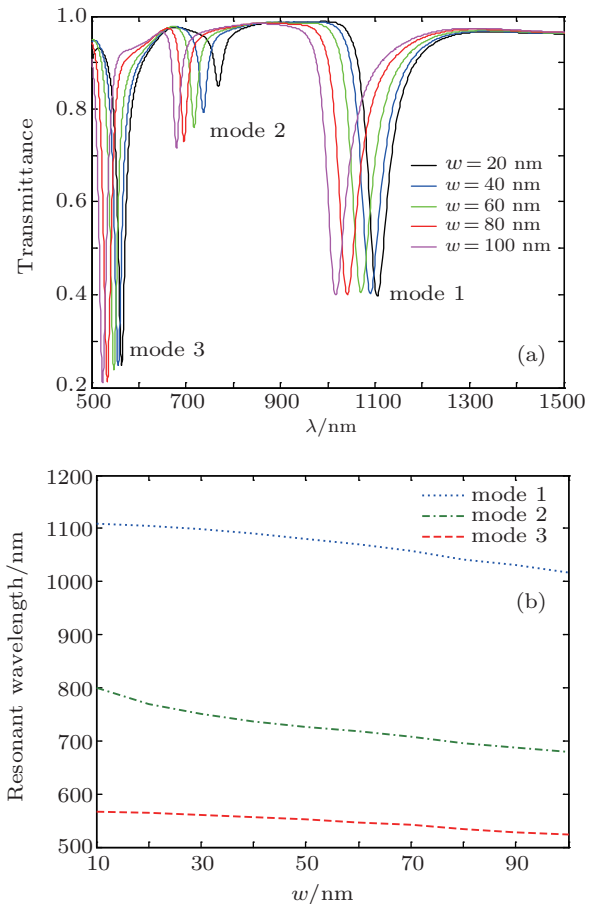


**Fig. 4.** (color online) (a) The transmittance of the filter with different wall widths, the resonant wavelengths move towards the short wavelength (blue shift) when  $w$  changes from 20 nm to 100 nm. (b) The dependence of the resonant wavelengths on the width of the metal wall.

To vividly illustrate the transmission characteristics of the SPPs, the electric field distributions are simulated with the FDTD method, as shown in Fig. 5. In the case of  $w = 40$  nm, the SPPs cannot pass through the filter at the transmission valleys of the three resonant modes, while easily pass through it at other wavelengths (959.08 nm for example). Thus, it is clear that the transmission spectrum of the filter can be tuned by varying the width of the metal wall.

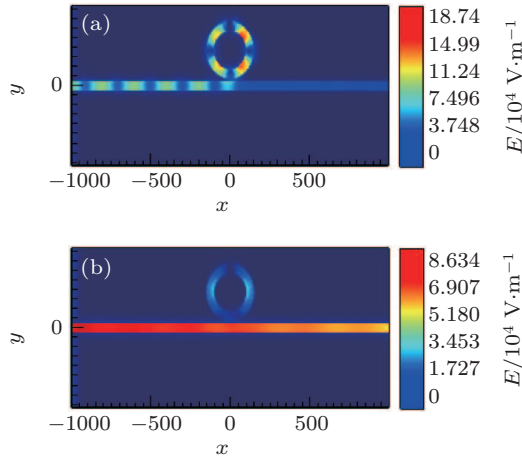


**Fig. 5.** (color online) (a) The electric field distribution at resonant wavelength 556.38 nm, the SPPs will be stopped in this case. (b) The electric field distribution at wavelength 959.08 nm on top of the curve, the SPPs can easily pass through the structure in this case. The width of the wall is set to be 40 nm in this study.

### 3.2. MIM band-stop filter with a circular split-ring resonator containing a linear medium

According to the details mentioned above, the resonant wavelength is determined by the effective length of the split ring and the effective refraction index of the SPPs. In this section, a linear medium is chosen to be the medium in the circular split-ring resonator, as shown in Fig. 6, and the refractive index is changed to study the transmission characteristics of the SPPs passing through the filter. The effective refraction index of the SPPs can be changed with the dielectric permittivity, thus the resonant wavelength can be tuned accordingly. The resonant wavelength is determined by the resonance condition described in Eq. (4). Replacing the permittivity of air  $\epsilon_0$  with that of the dielectric  $\epsilon_d$ , the dispersion relation can be expressed as

$$\tanh\left(\frac{h}{2}k_0\sqrt{n_{\text{eff}}^2 - \epsilon_d}\right) = -\frac{\epsilon_d\sqrt{n_{\text{eff}}^2 - \epsilon_m}}{\epsilon_m\sqrt{n_{\text{eff}}^2 - \epsilon_d}}. \quad (5)$$

Here the width of the wall is set to be 50 nm, the refractive index of the resonator is 1.0 (air), 1.1, 1.2, 1.3, and 1.4 respectively, and the medium in the bus waveguide is set to be air as before. The other parameters are the same as those in the previous sections.

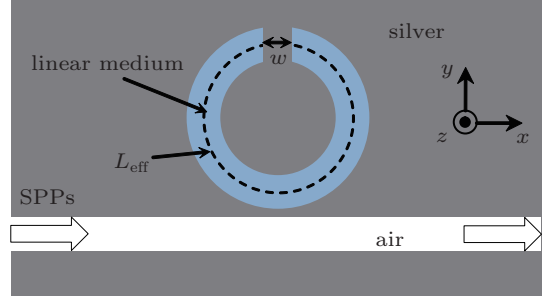


**Fig. 6.** (color online) Structure of the filter with a split-ring resonator filled with a linear medium.

The transmission characteristics of the SPPs propagating in the filter are plotted in Fig. 7(a). It can be seen that the resonant wavelengths move in the long-wavelength direction when the refractive index  $n$  varies from 1.0 to 1.4, which is called the red shift. Figure 7(b) shows the dependence of the resonant wavelengths on the refractive index of the resonator. The resonant wavelengths in the transmission spectrum can be tuned in a wide range by changing the refractive index, as shown in Fig. 7(b). With the width set to be  $w = 50$  nm, the electric field distributions are shown in Fig. 8 for  $n = 1.4$ . As an example, we choose one of the resonant wavelengths (652.17 nm) and a peak in the curve (1101.32 nm). It can be seen from this part that the resonance characteristics of the filter can be modulated by varying the refractive index of the medium, which relates to the dielectric constant.

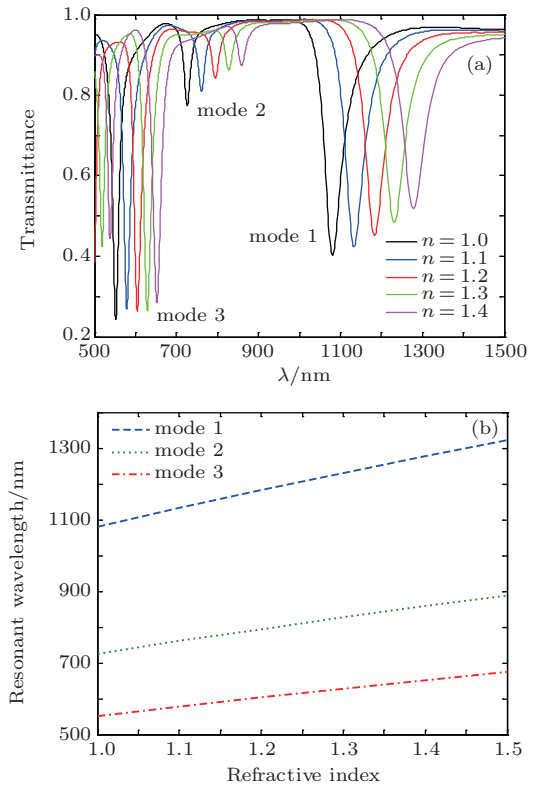


**Fig. 7.** (color online) (a) The transmittance with different refractive indices. Here the resonant wavelengths move in the long-wavelength direction when  $n$  changes from 1.0 to 1.4. (b) The dependence of the resonant wavelengths on the refractive index  $n$  of the medium.

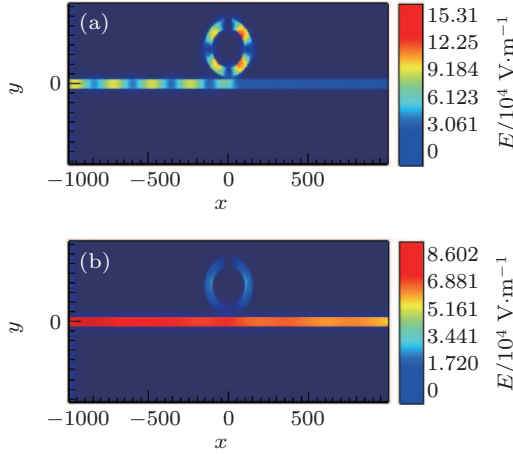


**Fig. 8.** (color online) The electric field distributions with the width of the wall set to 50 nm: (a) SPPs will be stopped at the resonant wavelength 652.17 nm; (b) SPPs can easily pass through the structure at the wavelength 1101.32 nm.

### 3.3. MIM band-stop filter with a circular split-ring resonator containing a nonlinear medium

As described in the previous section, the dielectric material affects the transmittance characteristics of the plasmonic filter at optical frequencies. To make use of this property and modulate the filter further, the linear medium is replaced by a nonlinear one. Here the electric field distribution can be considered as uniform except for the edge of the structure. The waveguide is considered to be lossless, and the dielectric layer is a Kerr medium characterized by linear permittivity  $\epsilon_l$  and a nonlinear part. Dielectric constant  $\epsilon_m$  changes with the intensity of the input light, as shown in the following expression:

$$\epsilon_m = \epsilon_l + \chi^{(3)} |E|^2, \quad (6)$$

where  $\epsilon_l$  is the linear dielectric constant, which is set to 2.25,  $\chi^{(3)} = 4 \times 10^{-18} \text{ m}^2/\text{V}^2$  is the third-order nonlinear susceptibility, and  $E$  is the electric field intensity of the input SPPs. The structure is shown in Fig. 9, the parameters are the same as those in the previous section except for the nonlinear medium in the resonator.

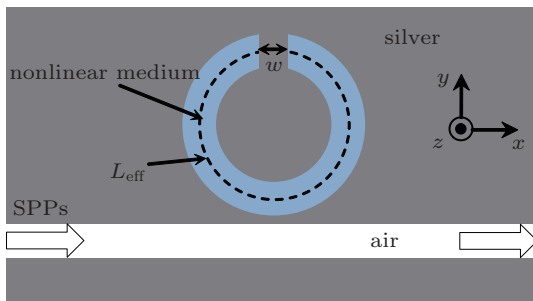


**Fig. 9.** (color online) Structure of the filter with a split-ring resonator containing a nonlinear medium.

It is similar to the linear medium that the wavelengths can be shifted by changing the refractive index of the medium. However, the dielectric constant depends on the intensity of

the incident light in the nonlinear medium as described in Eq. (6). So the refractive index can be changed by varying the intensity of the incident light conveniently. The transmission properties are described in Fig. 10, with the electric field intensity of the incident light  $E$  changed from  $1 \times 10^8 \text{ V/m}$  to  $5 \times 10^8 \text{ V/m}$ . The three modes of transmittance exhibit a red shift with increasing  $E$ , as shown in Fig. 10(a). The relationship between the resonant wavelengths and the input intensity is shown in Fig. 10(b). Taking  $E = 3 \times 10^8 \text{ V/m}$  for example, the three modes of transmittance are at 1376.17 nm, 921.66 nm, and 700.12 nm, respectively. Figure 11 shows the electric field distributions when SPPs passing through the filter at resonant wavelength 1376.17 nm, and the top of the transmittance curve at 1167.32 nm. It can be seen that the dielectric constant can be changed by varying the intensity of the input light indirectly to modulate the filter.

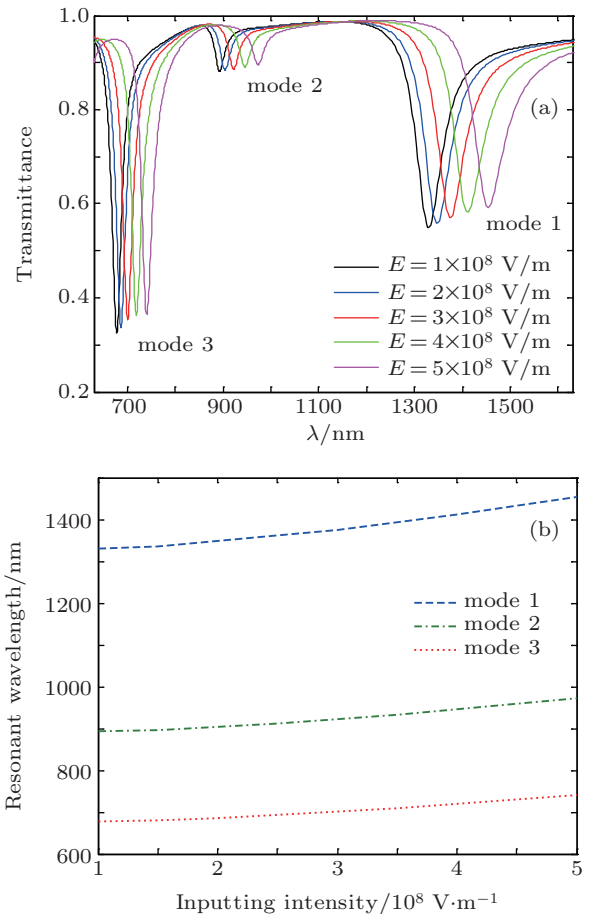


**Fig. 10.** (color online) (a) The transmission properties of SPPs propagating through the filter while changing the input intensity from  $1 \times 10^8 \text{ V/m}$  to  $5 \times 10^8 \text{ V/m}$ . (b) The dependence of the resonant wavelengths on the input intensity.

According to the above studies, these structures can be used as narrow-band filters, which can obviously tune the absorbing peaks of the plasmonic filters. It can be found that the bandwidth of the peak at a shorter wavelength is narrower than that at a longer wavelength, this is because the relative chang-



ing wavelength ( $\Delta\lambda/\lambda$ ) is greater for shorter wavelengths than that for longer ones.

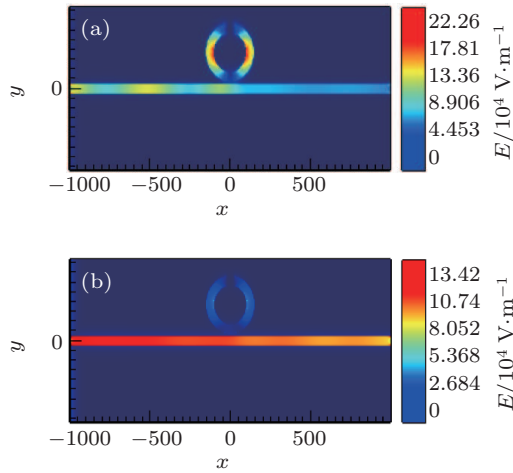


**Fig. 11.** (color online) The electric distributions of SPPs propagating through the filter: (a) SPPs will be stopped at 1376.17 nm which is one of the resonant wavelengths; (b) SPPs can pass through the structure easily at 1167.32 nm, which is a peak of the curve.

### 3.4. Transmission properties of filters with different positions of the metal wall

The previous three subsections show convenient methods to tune the transmittance spectrum of the plasmonic filter, and the filter can be tuned continuously in some appropriate situations. However, the transmittance of the SPPs is not sufficiently low at several resonant wavelengths, for example, mode 2 shown in Fig. 4(a), which is unsuitable for filtration. The position of the metal wall is changed to vary the transmission properties in this section. As shown in Fig. 12, we set an angle  $\theta$  between the radial direction of the gap and the original direction. The medium of the resonator is still air, the width of the wall is 50 nm, and the angle  $\theta$  is chosen to be  $0^\circ$ ,  $30^\circ$ ,  $45^\circ$ ,  $60^\circ$ , and  $90^\circ$  respectively.

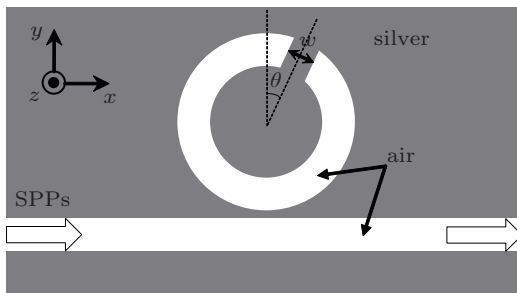


**Fig. 12.** Structure of the circular split-ring resonator with a variable angle.

The transmission properties with different angles are shown in Fig. 13. The resonant effect of mode 2 is poor when  $\theta = 0^\circ$ , as mentioned previously. By changing the angle to  $60^\circ$ , the band-stop characteristics of mode 2 become better. Figure 14 gives the electric field distributions at the resonant wavelengths, 1080.69 nm of mode 1 with  $\theta = 0^\circ$ ,

738.19 nm of mode 2 with  $\theta = 60^\circ$ , and 551.88 nm of mode 3 with  $\theta = 90^\circ$ . For mode 1, the angle between the two adjacent antinodes of the electronic field is  $180^\circ$ , with the resonance occurring unimpeded along these two directions which are called the effective directions, while being suppressed at other directions. For mode 2, there are three antinodes appearing in the electronic field where the resonance can be enhanced, and the angle between every two antinodes is  $120^\circ$ . For mode 3, there are four antinodes, and the angle between the nearest two antinodes is  $90^\circ$ . Thus, the split ring can be treated as a bended cavity, and the resonances in the resonator are similar to the standing waves. The two sides of the metal wall can be considered as the two ends of the cavity. For a given frequency, the number and the positions of antinodes and nodes of the electric field are invariable. The existence of the metal

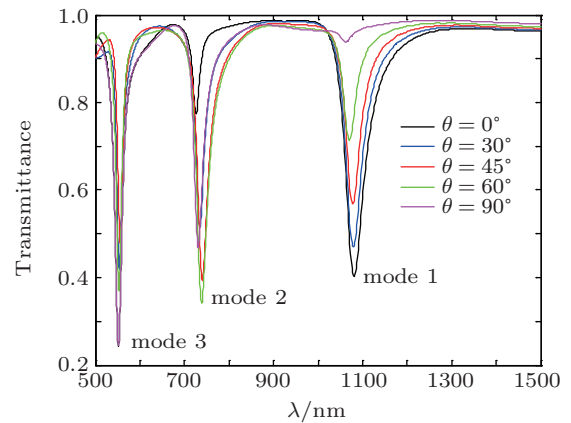


**Fig. 13.** (color online) The transmission spectra of the three modes at different angles  $\theta$ .

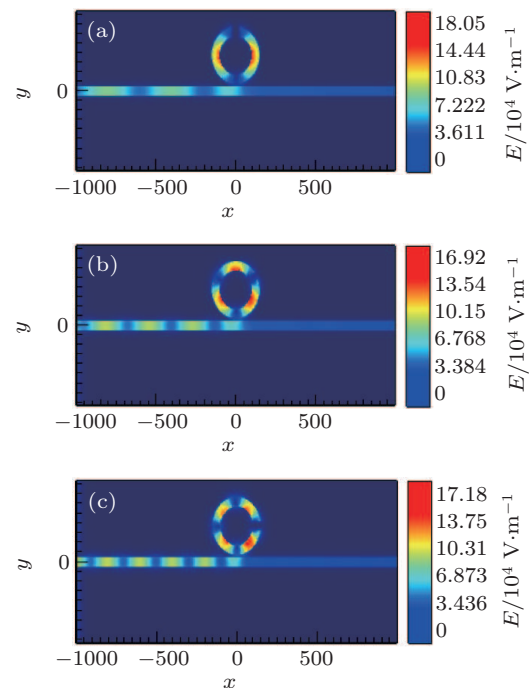


**Fig. 14.** (color online) The electric field distributions at resonant wavelengths: (a) 1080.69 nm of mode 1 with  $\theta = 0^\circ$ , (b) 738.19 nm of mode 2 with  $\theta = 60^\circ$ , (c) 551.88 nm of mode 3 with  $\theta = 90^\circ$ .

wall affects the standing waves. By placing the metal wall in the antinode, the balance of the standing waves is broken with the resonance suppressed and the strength of the absorption weakened. By changing the refractive index and the size of the gap, the frequencies at the absorption peaks can be varied in a wide range. Further, more effective directions can be found by changing the position of the gap. In other words, the requisite modes that cannot stop SPPs effectively can be improved by properly adjusting the direction angle  $\theta$ , and the resonant wavelengths can be chosen and enhanced selectively.

#### 4. Conclusion

In summary, a novel MIM band-stop filter with a circular split-ring resonator has been proposed in this paper, and the transmission properties at the resonant modes of SPPs passing through the filter have been simulated by using the FDTD method. By increasing the width of the metal wall, the resonant modes on the transmission spectrum move to the short wavelength, which is called the blue shift. The refractive index of the medium also affects the transmission properties of the SPPs. The resonant modes move to the long wavelength when the refractive index of the linear medium increases, which is called the red shift. When a nonlinear medium is used and the incident intensity is increased, the red shift occurs for the transmission properties of the SPPs. The strength of resonance can be improved by varying the position of the metal wall. The strengths at several requisite modes are enhanced as described in this paper by changing the angles between the radial direction of the wall and its original position. The transmission characteristics can be controlled easily by the above mentioned procedures, which can be used in potential applications for high-density optical integration.

#### References

- [1] Cai W, Wang L, Zhang X Z, Xu J J and Javier García de Abajo F 2010 *Phys. Rev. B* **82** 125454
- [2] Liu J Q, Wang L L, He M D, Huang W Q, Wang D Y, Zou B S and Wen S C 2008 *Opt. Express* **16** 4888
- [3] Zheng G G, Xu L H, Pei S X and Chen Y Y 2014 *Chin. Phys. B* **23** 034213
- [4] Pala R A, Shimizu K T, Melosh N A and Brongersma M L 2008 *Nano Lett.* **8** 1506
- [5] Han Z H, Liu L and Forsberg E 2006 *Opt. Commun.* **259** 690
- [6] Zhong R B, Liu W H, Zhou J and Liu S G 2012 *Chin. Phys. B* **21** 117303
- [7] Wang Y Q, Wang Y H, Zheng X H, Ye J S, Zhang Y and Liu S T 2014 *Chin. Phys. B* **23** 034202
- [8] Xiao S H, Liu L and Qiu M 2006 *Opt. Express* **14** 2932
- [9] Wang T B, Wen X W, Yin C P and Wang H Z 2009 *Opt. Express* **17** 24096
- [10] Okamoto H, Yamaguchi K, Haraguchi M and Okamoto T 2010 *J. Non-linear Opt. Phys.* **19** 583
- [11] Zhai X, Wen S C, Xiang D, Wang L L, Rexidaiguli W, Wang L and Fan D Y 2013 *J. Nanomater.* **2013** 484207
- [12] Yun B F, Hu G H and Cui Y P 2010 *J. Phys. D: Appl. Phys.* **43** 385102
- [13] Setayesh A, Mirnaziry S R and Abrishamian M S 2011 *J. Opt.* **13** 035004
- [14] Peng X, Li H J, Wu C N, Cao G T and Liu Z M 2013 *Opt. Commun.* **294** 368
- [15] Matsuzaki Y, Okamoto T, Haraguchi M, Fukui M and Nakagaki M 2008 *Opt. Express* **16** 16314
- [16] Lu H, Liu X M, Mao D, Wang L R and Gong Y K 2010 *Opt. Express* **18** 17922
- [17] Wang G X, Lu H, Liu X M, Gong Y K and Wang L R 2011 *Appl. Opt.* **50** 5287
- [18] Tao J, Wang Q J and Huang X G 2011 *Plasmonics* **6** 753
- [19] Yun B F, Hu G H and Cui Y P 2013 *Plasmonics* **8** 267
- [20] Hosseini A and Massoud Y 2007 *Appl. Phys. Lett.* **90** 181102
- [21] Zand I, Mahigir A, Pakizeh T and Abrishamian M S 2012 *Opt. Express* **20** 7516
- [22] Zand I, Abrishamian M S and Berini P 2013 *Opt. Express* **21** 79
- [23] Zheng G G, Su W, Chen Y Y, Zhang C Y, Lai M and Liu Y Z 2012 *J. Opt.* **14** 055001
- [24] Rakić A D, Djurišić A B, Elazar J M and Majewski M L 1998 *Appl. Opt.* **37** 5271